Recent subsidence of the northern Suez canal

In contrast to a recent interpretation of delta coast stability[1], we now show that the northeastern Nile delta in Egypt has been actively sinking relative to the sea during the recent Holocene epoch. The northern Nile delta is only about 1 m above sea level, making the northern Suez Canal and coastal cities of Port Said and Port Fuad (combined population nearly 500,000) highly vulnerable. Subsidence and world sea-level rises contribute to coastal erosion, incursion of salt in the groundwater underlying the delta plain, and silting problems in the canal entrances[2]. These processes must be considered when implementing protection measures for this area.

The entire Holocene sedimentary sequence has been recovered from Smithsonian core S-21 (total length, 49 m; elevation < 1 m), drilled in Port Fuad beside the northern canal bypass (Fig. 1). The early Holocene sediments comprise basal shell-rich sands identified as transgressive deposits from shallow marine to littoral origin. These are overlaid by a thick (47 m), typical Holocene deltaic offlap sequence (Fig. 1). Marine muds and delta-front sandy muds evolve upwards to sandy littoral and muddy lagoonal sediments.

Our study differs from earlier analyses[3,4] in that we dated sediments using accelerator mass spectrometric (AMS) ^{14}C analysis of individual shells, urchin fragments and wood, calibrating the dates to obtain calendar ages. We also took into account the water depth at the time of sediment deposition, estimated from an analysis of the fauna present (ostracod, foraminifera, mollusc). This is an important factor limiting the precision of subsidence-rate determination.

We obtained 11 AMS dates from core S-21 ranging from 6,480 ± 40 yr BP (radiocarbon dates are all calibrated calendric ages unless otherwise noted) at a depth of 45 m in the lower part of the Holocene mud section, to modern dates near the core top. There was a remarkably consistent pattern of sediment accumulation between 6,500 and 950 yr BP (at a depth of 14 m; Fig. 1). The upper 14 m of core section comprises a mixture of sandy shallow near-shore, strandline and coastal-ridge deposits — this inconsistency in the relationship between age and depth in the upper 14 m of sand is probably due to reworking during dredging of the Suez Canal bypass in the 1970s and 1980s.

Near the base of core S-21 (at a depth of 47 m), there is a marked unconformity (or break) between the top of the transgressive sands and the immediately overlying marine prodelta muds. Sands at a depth of 48 m (1 m below the sand–mud contact) are dated to 8,540 ± 150 calendar yr BP by conventional ^{14}C analysis of bulk-sample carbonate. This date is comparable to that of a sample near the top of transgressive sands in core Fadda-1 to the south (9,020 ± 330 calendar yr BP; uncalibrated age 8,480 ± 280 yr BP, at a depth of 42 m)[5]. Dates in both cores indicate a hiatus of up to 1,000 years.

Littoral shell-rich sands present at 48 m (~8,500 yr BP) and 14.6 m (~950 yr BP) were deposited at a water depth of 0–10 m, whereas the fauna in the muds at 45 m (6,480 yr BP) represents water depths of > 10 m (ref. 6). At 8,500 yr BP, sands were deposited at a depth of 0–10 m below a sea level which, taking a rise in eustatic sea level[7] into account, was ~14 m below the present level; that is, 14–24 m below the sea

level at the time. At 6,500 yr BP, these sands were 3 m below the sediment surface, which was being deposited at a depth > 10 m at a time when sea level was ~6.5 m below present. Thus the 8,500-year-old sands would have sunk by that time to a depth of at least 19.5 m below present sea level.

Similar reasoning places these sands at a depth of 34.5 to 44.5 m below present sea level at 950 yr BP (0.5 m lower eustatic sea level + 34 m overlying sediments + 0–10 m water depth). At present, the sands lie at 48 m below sea level.

From this analysis we calculate a mean subsidence rate of 3.98 mm per year from 8,540 years ago to the present. Thick Holocene sediments in cores P.S.16-1979 (in Port Said)[3] and Fadda-1 (ref. 5) at 46.5 m and 42 m, respectively, indicate similar subsidence rates. In addition to long-term subsidence, the absolute sea level is rising at roughly 1.0–1.5 mm per year[7,8], so current relative sea-level rise in this area is at least 5 mm per year. Independent analysis of the 1923–1946 tide-gauge record at Port Said shows a relative sea-level rise of 4.8 mm per year[9].

The accumulation rate of muds during most of the Holocene (5.4 mm y^{-1}) is quite
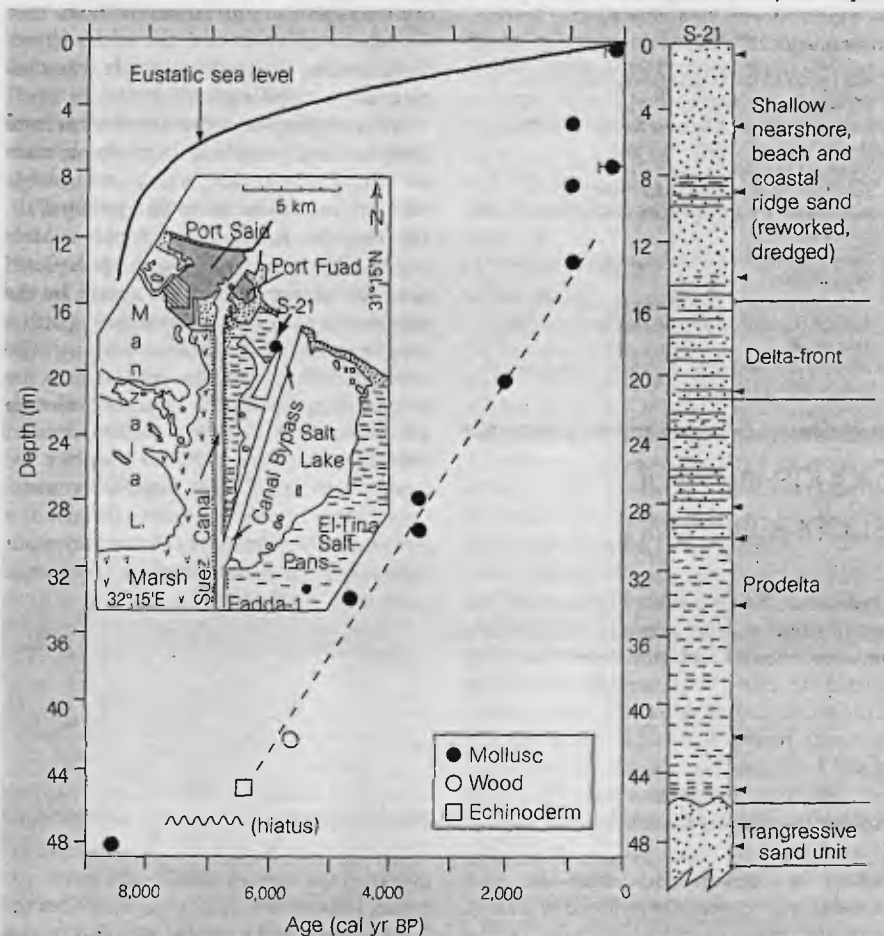

Figure 1 Calibrated radiocarbon dates (for $\Delta R = 0$; that is, the worldwide value for the marine radiocarbon reservoir age, R, is assumed) from Nile delta core S-21, in relation to depth. Error bars (1σ) fall within the symbols except where shown. The dashed line shows the age–depth trend for 14–45 m depth, and the solid line is the eustatic sea-level curve[7]. Simplified core log (right) is from refs 3 and 6. Inset shows the core location in the northeastern Nile delta.

constant (dashed line, Fig. 1). After the deposition of littoral sands at 8,500 yr BP, inundation due to rapid sea-level rise allowed the accumulation of muds at a rate exceeding subsidence. Starting at 950 yr BP, more rapid accumulation of sands (~15 mm yr^{-1}) brought the sediment level up to sea level, and allowed deposition to keep pace with subsidence.

The main cause of subsidence in this delta region is ongoing faulting, as well as downwarping, of the underlying 3000 m of Late Miocene to Quaternary sequences[10]. The whole northern Nile delta plain has been lowered north of a flexure roughly 30 km inland from the coast[2]. Vertical displacement of our dated Holocene sediments provides the most accurate means to measure long-term subsidence, rates of relative sea-level rise and recent sediment accumulation in this region.

Daniel J. Stanley
Deltas-Global Change Program,
Smithsonian Institution,
Washington DC 20560, USA
e-mail: stanley.daniel@nmnh.si.edu
Glenn A. Goodfriend
Geophysical Laboratory,
Carnegie Institution of Washington,
*Washington DC 20015, USA*

1. Said, R. *The River Nile: Geology, Hydrology and Utilization* (Pergamon, New York, 1993).
2. Stanley, D. J. & Warne, A. G. *Science* **260**, 628–634 (1993).
3. Stanley, D. J. *Science* **240**, 497–500 (1988).
4. Stanley, D. J. *Mar. Geol.* **94**, 147–154 (1990).
5. Sneh, A. *et al. Quat. Res.* **26**, 194–206 (1986).
6. Bernasconi, M. P., Stanley, D. J. & DiGeronimo, I. *Mar. Geol.* **99**, 29–43 (1991).
7. Lighty, R. G., Macintyre, I. G. & Stuckenrath, R. *Coral Reefs* **1**, 125–130 (1982).
8. Zerbini, S. *et al. Global Planet. Change* **14**, 1–48 (1996).
9. Emery, K. O., Aubrey, D. G. & Goldsmith, V. *Mar. Geol.* **81**, 41–52 (1988).
10. Neev, D. *et al. Israel Geol. Surv. Rep. MG/73/5* 1–43 (Israel Geol. Surv., Jerusalem, 1973).

Clouds without supersaturation

Traditional Köhler theory[1] describes the equilibrium vapour-pressure relationship between liquid solution particles and humid air. Here we present the concept of multiphase–multicomponent Köhler theory, which reveals that stable cloud droplets of size 1–10 μm could exist in air with a relative humidity of less than 100%. This may explain the occurrence of persistent large-droplet fogs or smogs such as previously existed in London and which are now found in various heavily polluted locations, near the exits of chimneys and in the plumes of volcanoes.

Assumptions are usually made, explicitly or implicitly, that the solute mass in a droplet is fixed as it grows in size. The result is that a critical size exists at which the

Figure 1a, Conventional Köhler curve for a 30 nm dry particle consisting of ammonium sulphate at 298 K. **b,** A similar particle containing an additional, insoluble 500 nm core (the amount of ammonium sulphate is the same as with a). The effect of insoluble material has been studied in detail[7]. **c,** Particle containing a slightly soluble 500 nm core. The solubility used[6] (0.00209 g cm^{-3}) corresponds to that of CaSO$_4$. The sharp minimum of the curve shows the point at which all of the core is dissolved. CaSO$_4$ particles occur commonly in air, and dissolved CaSO$_4$ has been found in fog-water collected in the Po Valley, Italy[9]. **d,** Effect of an added, highly soluble gas, nitric acid. Initial gas-phase concentration of HNO$_3$ was 1 p.p.b.v., and the Henry's law constant used[10] (mole-fraction scale) was 853.1 atm^{-1}. Because nitric acid is allowed to deplete from the gas as it is absorbed by the droplets, the term $b_a(r)$ in equation (1) depends on the aerosol number concentration, which in this case was assumed to be 100 cm^{-3}. Aerosol size distribution was taken to be monodisperse (a qualitatively similar curve would result if the aerosol population was 1,000 cm^{-3} and initial HNO$_3$ concentration 3 p.p.b.v.). The smooth minimum in the curve is caused by the depletion.
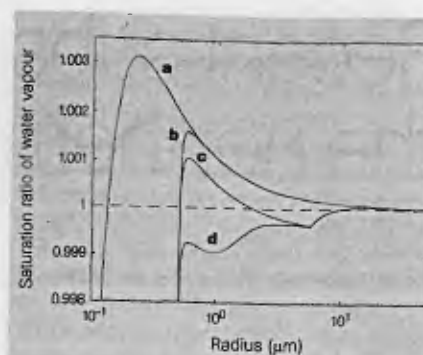
Raoult effect (depression of vapour pressure due to dissolved substance) just balances the Kelvin effect (increase of vapour pressure due to droplet curvature). Above that size, a droplet is said to be activated and will grow spontaneously if the ambient supersaturation remains at or above the respective equilibrium value. However, this ordinary Köhler formulation does not describe droplets in which the solute derives from either slightly soluble aerosol particles[2] or soluble gases[3,4].

We consider a situation in which aerosol particles containing both hygroscopic matter (salt) and a weakly soluble or insoluble core, are suspended in humid, polluted air. The particles absorb water, highly soluble gases such as nitric acid (which are depleted from the vapour due to the uptake by the particles), and weakly soluble gases (with a roughly constant gas concentration). The weakly soluble core is assumed to keep the surrounding liquid as a saturated solution until it has fully dissolved. At equilibrium, the saturation ratio of water vapour (S) equals the equilibrium vapour pressure ($p_{sol,w}$) of water over a solution droplet of a given radius (r) divided by the water vapour pressure over a plane surface ($p_{s,w}$), which is given by:

$$S = \frac{p_{sol,w}}{p_{s,w}} \qquad (1)$$

$$\approx 1 + \frac{a}{r} - x_{ws} - x_{wg} - \frac{b_s}{(r^3 - r_0^3)} - \frac{b_a(r)}{(r^3 - r_0^3)}$$

Here r_0 is the radius of the core, a/r describes the Kelvin effect, x_{ws} and x_{wg} are the mole fractions of the weakly soluble species originating in the aerosol particle and in the gas phase, respectively, $b_s/(r^3 - r_0^3)$ describes the Raoult effect of the soluble salt, and $b_a(r)$ is the term accounting for the highly soluble, condensing trace gas[5].

Figure 1 compares the traditional Köhler curve to the more complete multiphase–multicomponent theory. The particle sizes

and compositions are selected as realistic examples as are the concentrations of water-soluble gases. We have not included in the curves the effect of a slightly soluble gas. For simplicity, we assume that the highly soluble substances do not influence the solubility of the weakly soluble substances (a conservative approximation). What becomes evident is that the combination of the amount of solute from the soluble gas and/or the slightly soluble aerosol particle, along with the vapour pressure reduction due to the Kelvin effect for the increased initial size of the slightly soluble particle, may be sufficient to keep the saturation ratio below unity for droplet sizes up to ~10 μm. In retrospect, this result is evident in the traditional simple formulation of the Köhler equation[6]:

$$S = 1 + \frac{a}{r} - \frac{b}{r^3} \qquad (2)$$

because $S < 1$ if $b/r^3 > a/r$, which simply depends on the magnitudes of a and b. What we have pointed out is that realistic particle sizes, particle solubilities and gas concentrations exist to cause this to happen. In fogs formed by these processes, the cloud-drop-sized particles are thermodynamically similar to submicrometre 'haze' particles. However, without sophisticated physicochemical methods, they are physically indistinguishable from classical, 'activated' drops.

Markku Kulmala, Ari Laaksonen
Department of Physics, PO Box 9,
FIN-00014, University of Helsinki, Finland
e-mail: kulmala@phcu.helsinki.fi
Robert J. Charlson
Departments of Atmospheric Sciences
and Chemistry,
University of Washington,
Box 351700 Seattle, Washington 98195, USA
Pekka Korhonen
Finnish Meteorological Institute,
Air Quality Department, Sahaajankatu 20 E,
FIN-00810, Helsinki, Finland